NOTICE CONCERNING COPYRIGHT RESTRICTIONS

Lithologies, Hydrothermal Alteration, and Rock Mechanical Properties in Wells 15-12 and BCH-3, Bradys Hot Springs Geothermal Field, Nevada

Susan Juch Lutz[1], Ashwani Zutshi[1], Ann Robertson-Tait[2], Peter Drakos[3], and Ezra Zemach[3]

[1]TerraTek, A Schlumberger Company, Salt Lake City UT
[2]GeothermEx, A Schlumberger Company, Richmond CA
[3]ORMAT Nevada Inc., Reno NV
SLutz@slb.com

Keywords

Enhanced geothermal system, petrology, X-ray diffraction mineralogy, argillic and phyllic alteration, core permeability, petrophysical properties, compressive strength, Mohr-Coulomb failure envelopes, sliding friction, shear failure

ABSTRACT

In the Bradys Hot Springs geothermal field of northwestern Nevada, Well 15-12 has been selected as a candidate well for mechanical and chemical stimulation as part of an enhanced geothermal system (EGS) demonstration project (U.S. Department of Energy project with Ormat Nevada and GeothermEx). Well 15-12 has recently been drilled and logged, and is an attractive candidate for EGS work with downhole temperatures of 400°F (204°C) in metamorphic basement rocks. This non-commercial well is close to the Bradys Fault and has similar formations as production wells in the northern part of the field, but injection tests show an injectivity index of less than 1 gpm/psi, and no significant circulation losses in the basement from the casing shoe at 4,245 ft to the total depth (5,096 ft). Although no core is available from 15-12, companion core samples are available from the target stimulation interval owing to the presence of a fully cored well (BCH-3) drilled on the 15-12 pad.

Preliminary tasks of the EGS program are to characterize the rocks transected by the candidate well with an emphasis on texture and basic lithotypes, alteration and clay mineralogy, the natural fracture and vein system, and geomechanical character of various rock units. To this end, X-ray diffraction (XRD) mineralogical analyses and petrologic analyses of well cuttings from 15-12 and corresponding whole core samples from BCH-3 cores were performed. Core samples from BCH-3 were selected for determination of basic core properties (density, porosity, and permeability) and mechanical testing to determine rock strengths and other elastic properties. These measurements will be used in the design of hydraulic and chemical stimulation activities in Well 15-12.

Core analyses on the BCH-3 core samples indicate generally high ambient porosities (8-10%) but low permeabilities (<0.01 md) for the rhyolites. The metamorphic samples have less than 2% porosity and negligible permeability. Rock mechanical tests on the core were conducted to determine mechanical properties of the various lithologies including: radial versus axial volumetric strain, stress-strain relationships, dynamic versus static Young's moduli, and frictional strengths and failure responses under a variety of confining conditions and temperatures. The mechanical test results indicate moderately high rock strengths; with unconfined compressive strength estimates of 240-275 MPa for the more siliceous lithologies, and 70-194 MPa for argillically-altered rhyolites and chloritic metavolcanic rocks. Effective compressive strengths range from 220 Mpa at 1 MPa confining pressure for crystal-supported rhyolite, and 37 MPa at 1 MPa confining pressure for sericitized metamorphic rocks at the top of the basement, up to 304 MPa at 20 MPa confining pressure for pebbly meta-volcaniclastic rocks. At temperatures of 200°C, quasi-static values for Young's moduli range from 48 to 55 GPa (in crystal-rich rhyolite tuffs) up to 60-76 GPa (in the metamorphic rocks); Poisson's ratios range from 0.10 to 0.29.

The results of the laboratory tests were used to construct Mohr-Coulomb failure envelopes for the proposed reservoir rocks, and to evaluate the propensity for frictional failure along natural fractures in the open-hole interval of Well 15-12. At 200°C, sliding friction angles for the residual effective compressive strength range from 29.1° to 43.7°. Corresponding coefficients of sliding friction values range from 0.56 in chlorite-altered meta-basalt, up to 0.98 in clast-supported meta-volcaniclastic rocks. The metamorphic rocks in the open-hole interval of 15-12 have abundant veins, clayey shear planes, and other planar features that may be amenable to shear stimulation under higher wellhead fluid pressures. Hydraulic stimulation of the well is intended to enhance formation permeability through self-propping shear failure along the most optimally oriented and critically stressed of these pre-existing features.

Introduction

The objective of the Bradys Enhanced Geothermal System (EGS) project is to increase power generation at the Bradys

power plant by stimulating a well or wells in the southwestern part of the field, along the extension of the Bradys fault south of the production area (Figure 1). This will be accomplished by stimulating Well 15-12, enabling it to be used either as a production well (directly providing additional power) or an injection well (sweeping more heat toward existing producers and thus enhancing their productivity).

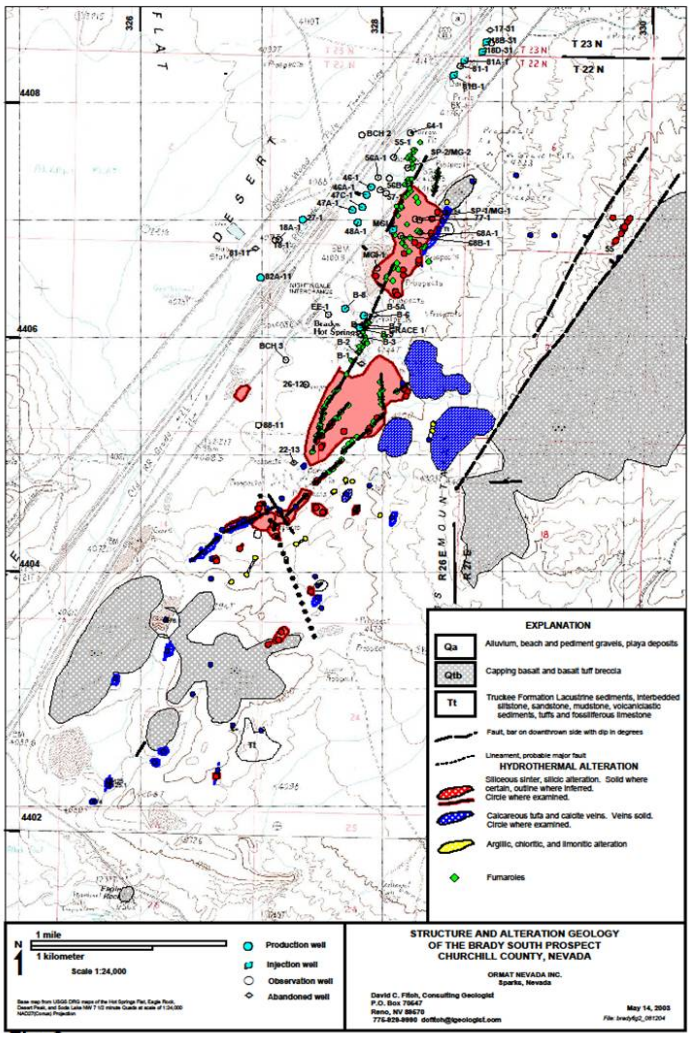

Figure 1. Well locations, faults, and surface thermal features, Bradys Hot Springs geothermal project, Nevada. The proposed EGS (Enhanced Geothermal System) target well is 15-12; located on the BCH 3 well pad.

There are several EGS options available for this area at Bradys, all of which include hydraulic and perhaps chemical stimulation of Well 15-12. Well 15-12 is an attractive candidate for EGS work in that downhole temperatures of 400°F (204°C) have been measured, and a wellbore image log has been acquired. Furthermore, core samples are available from the target interval owing to the presence of a fully cored well (BCH-3) drilled on the 15-12 pad (within 50 feet of 15-12).

Bradys production wells generally range in depth from 2,000 to 5,000 feet and produce from Tertiary lavas near the Bradys fault zone (mainly the Chloropagus Formation, although production has also been found in deeper wells in the Rhyolite Unit). Injection wells are about 1,000 feet deep, and target an andesite flow near the top of the Desert Peak Formation, again adjacent to or within the Bradys Fault zone. The stratigraphy at Bradys is very similar to that at Desert Peak (Benoit et al., 1982), and includes Truckee Formation unconformably overlying Tertiary volcanic rocks of the Desert Peak and Chloropagus Formations, a 'Rhyolite Unit', and metamorphic basement rock of varying lithologies consistent with the so-called 'pT2' unit identified at Desert Peak (Lutz et al., 2004; Lutz et al., 2009). Hematitic metavolcanics in the basement are associated with the mid-Jurassic Humboldt Mafic Complex (Johnson and Barton, 2000; Lutz and Hulen, 2001).

The formations encountered in Well 15-12 are typical of the Bradys field, and include about 400 feet of Truckee Formation underlain by a thick section of Tertiary volcanic rocks. Well 15-12 is cased to below the Rhyolite Unit, and the underlying metamorphic basement is characterized by slow drilling, and extensive mineralization, veining and fracturing. Preliminary analysis of a wellbore image log (Schlumberger's Formation Micro Imager FMI™) through this section shows extensive fracturing in the basement, although the fractures appear to be mostly sealed by later mineralization. There were intermittent or partial losses between 4,600 and 4,800 feet; however, these show little or no 'character' on the temperature profiles and therefore no significant permeability is likely to exist. This conclusion is also supported by injection test data, which show an injectivity index of less than 1 gpm/psi. There were no circulation losses in the basement rocks from the casing shoe at 4,245 to 4,600 feet, nor from 4,800 feet to TD.

Preliminary tasks of the EGS program are to fully characterize the rocks transected by the candidate wells with an emphasis on the natural fracture and vein system and the geomechanical character of various rock units. To this end, XRD mineralogical analyses and petrologic analyses of cuttings from the open-hole interval of 15-12 and corresponding whole core samples from BCH-3 cores were performed. Core samples from BCH-3 were selected for determination of basic core properties (density, porosity, and permeability) and mechanical testing to determine rock strengths and other elastic properties. These measurements will be used in the design of hydraulic and chemical stimulation activities of well 15-12. This paper discusses the fundamental properties of the rock types in well 15-12 as the building blocks of the geological and geomechanical model to be used for the reservoir stimulation plans.

Lithologies and Hydrothermal Mineral Zoning in Well 15-12

Systematic sampling and X-ray diffraction analysis of cuttings from Well 15-12 (every 100-200 ft) reveals mineralogical changes related to rock type and to the type of hydrothermal or metamorphic alteration (Figure 2). A variety of low-temperature clay and zeolite minerals with well-defined zoning patterns are present within the Tertiary volcanic rocks (Figure 3). Below near-surface opaline sinter deposits and Plio-Pleistocene lacustrine carbonates, basaltic andesites of the Miocene Chloropagus Formation are variably clay-altered. This argillic alteration zone extends to a depth of 2,000 ft and is characterized by abundant smectite and mixed-layer chlorite-smectite, moderately abundant

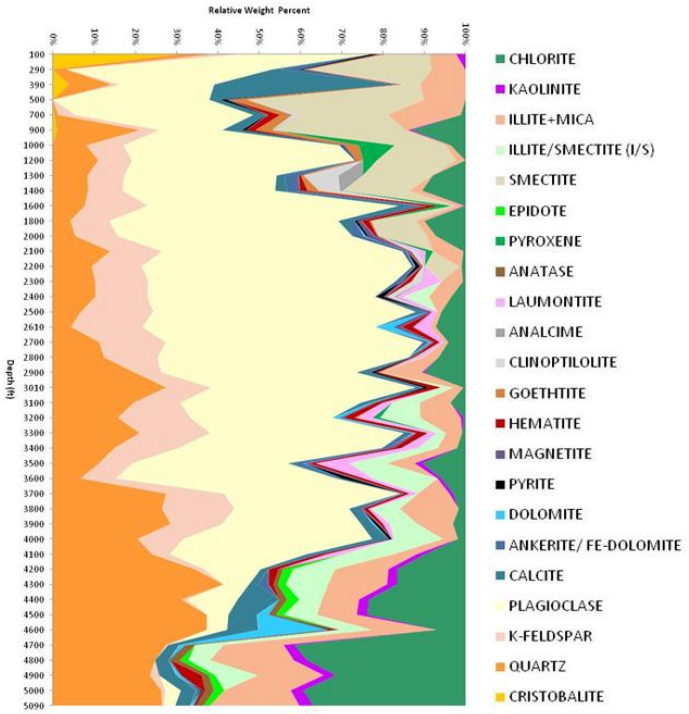

Figure 2. Whole-rock X-ray diffraction mineralogy for well cuttings samples from Well 15-12. The contact between Tertiary volcanic rocks and pre-Tertiary meta-volcanic rocks in the metamorphic basement occurs at approximately 4,100 ft. Abundant potassium feldspar characterizes devitrified rhyolite ash flow tuffs in the Tertiary volcanic section, and increased quartz contents, abundant chlorite and minor kaolin (serpentine) minerals are indicative of metamorphic lithologies.

low-temperature zeolites such as clinoptilolite and analcime, and iron-bearing carbonate veins and amygdule-fills composed of chalcedonic quartz, ferroan calcite, siderite and ankerite. These minerals are consistent with present-day temperatures at these depths within the well and define clayey lateral seals and 'caprock' on the modern geothermal system at Bradys.

The contact between andesite flows at the base of the Chloropagus Formation and underlying Oligocene ash flow tuffs occurs at about 2,100 ft. Here, the presence of epidote veins and epidote-rich gouge material possibly suggest the presence of a large-displacement normal fault that has uplifted footwall lithologies to this relatively shallow depth. This fault is likely the subsurface expression of the Bradys fault mapped in surface exposures (Faulds and Garside, 2003), and similar to a fault in the BCH-3 core at 2,081 ft described by Faulds and Hinz (2003) as dipping at 58°. In Well 15-12, the fault defines the sharp contact between the smectite and mixed-layer illite-smectite (I/S) clay alteration zones, and also coincides with the uppermost occurrence of the higher temperature zeolite, laumontite. At the top of the I/S alteration zone, the mixed-layer clay has 50-60% smectite interlayers and is joined by moderate chlorite alteration of dacite flows in the middle of the Rhyolite Unit.

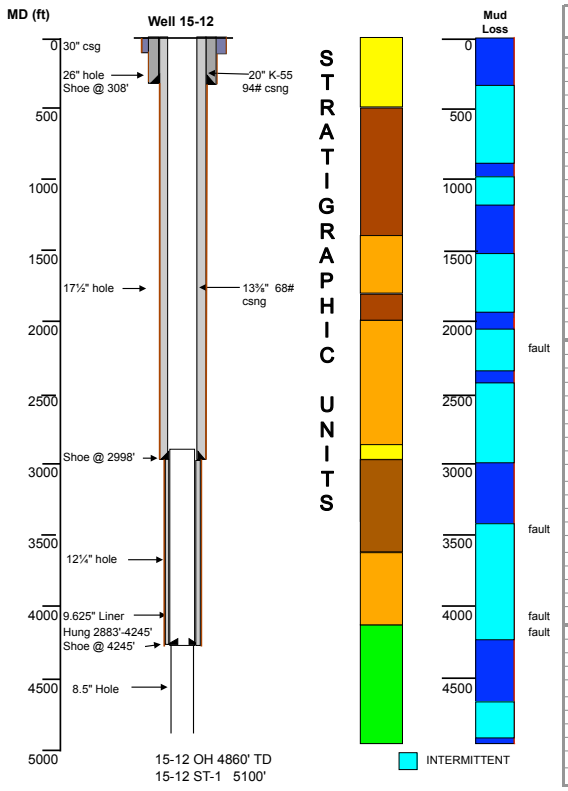

CR	QTZ	KF	CAL	DOL	PY	HEM	CLIN	ANA	LAU	SM	CHL/SM	IL/SM	KA	IL	CHL	EP	TOUR	Zone
XXX							X			X			X					Argillic
			XX	X	X					XX								
				XX	X		X			XX								
			XXX							X								
			X		X					XXX								
							X			XXXX								
			X			X	X			XX								
			X			XX	X			XX								
	XX		XXX		X	XX				XXX	XX		X					
						X				X	X							
	XX		X		X					X	X							
	XX									XX								
			X	XX		X	XXX	XX		XX	X							
			X	XX		X	XX	XX		XX	XX							
		X	XXX	XX		X				X	X							
		XXX		XX	X					XX	XX							
			XX		X					XX	XX							
					X					XX	XX							
				XXX	X					XX	X							
	XX	X		X			X		X							X		Argillic/Phyllic
				X			X			X	X							
		X		X			X		XX			X						
		X			X		X	X	X		X	X						
			X	X					X		X							
				XXX		X			XX		X							
	X	X		X		X			X		X							
	X	X							X		X							
	XXX		X	X	X	X					XX							
	XXX	X	X	X		XX						X						
	XXX	X	X	X		X			X		X	XX						
	XX	XXX		X		XX			XX			XX	X					
	XXX	XXX	X	X		XX			X		X	X						
	X	XX		X		X			XX		X	X						
	X		X	XX		X			XXX		XX	XX						
			X		XX	X			X		X	XXX						
	XXX	X				X			X		X							
	XX	XX	X	X		X			X		X	XX						
	XXX		XX	X		X			X		X	XX						
	XX		XXX		X				X		X	XXX						
	XX		XX	X		X			XX			XXX	X	XX	XX			Metamorphic
	XXXX	XX	XX	XXX		X						XX	X	XX	XXX	X		
	XXXX		X	X		X						XXX	X	XX	XXX	X		
	XXX		XXX									X	X	X	XXX	XX		
	XXXX		XX	XX								X	X	XX	XXX	X		
	XXXX		XX	XXX	X							X		XX	X			
	XXX		XX	X								X	X	XX	XXXX			
	XX		XX									X	X	XX	XXXX	X		
	XX		XXX	X		XXX						X	X	XX	XXX	X		
	XXX		XXX	X		XXX							X	XX	XXXX	XX	X	
	XXX		XXX	X		XXX							X	XX	XXXX	X	X	

Figure 3. Completion, general stratigraphy, circulation losses, interpreted faults, and secondary alteration minerals in Well 15-12. The shallow argillic alteration zone (100 - 2,200 ft) is characterized by smectite, mixed-layer chlorite-smectite, clinoptilolite, analcime, and calcite. The argillic/phyllic alteration zone (approximately 2,100 - 4,100 ft) is characterized by mixed-layer illite-smectite, laumontite, dolomite, pyrite, and hematite. Below 4,100 ft, the secondary mineralogy consists of metamorphic minerals including quartz, serpentine, illite and muscovite, chlorite, epidote, and tourmaline. The locations of faults are based on the presence of fault gouge in the 15-12 well cuttings samples, and descriptions of the BCH-3 core by Faulds and Hinz (2003).

Devitrified rhyolite ash flow tuffs are present from 3,700 ft to the top of the basement at about 4,100 ft. The tuffs are slightly to moderately siliceous with 20-30% total quartz and moderately clay-altered. Illite-smectite clays (I/S) in the tuffs have 20-30% smectite interlayers. With depth, X-ray diffraction analyses of clay-sized separates (less than 4 micron size fraction) document a consistent decrease in the amount of interlayered smectite in the I/S clay. The amount of interlayered smectite is related to paleo-temperatures in the Bradys geothermal history. At the top of the I/S zone at 2,400-2,900 ft, the mixed-layer clay is smectite-rich with up to 60% smectite interlayers, indicating formation of the I/S clay at about 180°C. Closer to the basement contact, the I/S clay has 20-30% smectite interlayers, suggesting slightly higher paleo-temperatures in the 180-200° C range.

General lithologies: volcanic and sedimentary (yellow), basalt and andesite (brown), rhyolite and dacite (orange), and meta-volcanics (green). Mineral abbreviations: CR-cristobalite; QTZ-quartz; KF- potassium feldspar, CAL- calcite; DOL- dolomite; PY- pyrite; HEM- hematite; CLIN- clinoptilolite; ANA- analcime; LAU- laumontite; SM- smectite; CHL/SM- mixed-layer chlorite-smectite; IL/SM- mixed-layer illite-smectite; KA- kaolinite and serpentine; IL – illite; CHL- chlorite; EP- epidote; TOUR- tourmaline.)

The base of the Tertiary section is faulted and probably in fault contact with the metamorphic basement between 4,000 ft and 4,100 ft in the Well 15-12 cutting samples, and at a core depth of 4,134 ft in the BCH-3 corehole. In both 15-12 and BCH-3, the top of the metamorphic basement is characterized by strong sericite alteration indicating prolonged exposure and weathering of the basement rocks before burial by the Oligocene ash flow tuffs. Minor overprinting of I/S geothermal clay extends down to a depth of 4,800 ft indicating at least some paleo-circulation of geothermal fluids within the upper part of the basement. The circulation of geothermal fluids produced this clay that now seals pre-existing fractures or open pores in this interval, contributing to the overall low permeabilities of these rocks.

The metamorphic rocks are composed of hematite-bearing metavolcanics associated with the mid-Jurassic Humboldt Mafic Complex. These rocks are moderately siliceous with 30-40% quartz and have undergone minor to moderate propylitic alteration (epidote-chlorite assemblages). Porphyritic andesite flows and pebbly volcaniclastic mudstones are extensively recrystallized and altered, and are now composed of up to 40% chlorite and 20% illite and muscovite (sericite). A variety of vein types are associated with the Humboldt Mafic Complex, and the veins and rocks were together variably sheared or deformed. Below TD in the 15-12 OH (4,860 ft), well cuttings from 4,800-5,090 ft in Sidetrack 1 are highly deformed to foliated fine-grained metasedimentary rocks with abundant chlorite. Throughout the meta-volcanic rocks, older vein assemblages include epidote-chlorite, actinolite-chlorite, tourmaline, and quartz veins. Younger veins of unknown age consist of less deformed coarsely crystalline calcite with hematite selvages throughout the basement, as well as open-space filling prismatic quartz at 4,300 ft.

Well 15-12 has 850 feet of open hole in the competent, fractured metamorphic rocks with sub-commercial permeability, and a total depth (TD) of 4,860 ft (5,096 ft in Sidetrack 1). The metamorphic rocks in the open-hole interval have abundant veins, clayey shear planes, and other planar features that may be amenable to shear stimulation under higher wellhead fluid pressures. Hydraulic stimulation of the well is intended to enhance formation permeability through self-propping shear failure along the most optimally oriented and critically stressed of these pre-existing features.

Rock Mechanics and Core Testing

Mechanical and petrophysical property analyses were conducted on selected core samples collected from Well BCH-3. The testing program consisted of:

- Continuous strength profiling of all rock types within the core segments using TSI™ scratch-testing apparatus;
- Drained triaxial compression testing on suites of elevated temperature vertical samples for Mohr-Coulomb failure envelope delineation with simultaneous ultrasonic velocity measurements to determine dynamic mechanical properties; and
- Basic petrophysical properties (i.e., density, porosity and permeability at ambient stress conditions).
- Pulse-decay permeability testing under a variety of confining conditions for the original core plugs and the fractured plugs after triaxial compression testing.

Ormat Technologies Inc. provided eleven core segments from the BCH-3 core; six within the Tertiary volcanic section (Samples DEP1-DEP6; 3567-4127 ft), and five from the metamorphic basement (Samples DEP7-DEP11; 4207-4863 ft) (Table 1). The purpose of the testing was to provide the following:

- Semi-quantitative empirical information on variations in unconfined compressive strength with lithology and extent of veining, and an overall assessment of rock heterogeneity using scratch testing.
- Strength and rock physics information for developing a failure model for the material. With adequate measurements of strength on core samples and with the availability of supplementary information such as clay content, sonic velocity, and porosity, logging-based predictions of in-situ strength may be possible. With such information, predictions of borehole stability and stress conditions can be performed.
- Static and dynamic mechanical properties that can be used in concert with well logs for predicting reservoir response during hydraulic stimulation and injection/production and for creating 3D stress models (e.g., Davatzes and Hickman, 2009; Hickman and Davatzes, 2010).

Results of Mechanical Testing

Triaxial compression tests were conducted on cores from BCH-3 using a servo-controlled testing apparatus that subjected the samples to the desired stress states at controlled strain rates. Prior to testing, each test sample was placed between two end-caps and jacketed with either a Teflon or polyolefin sleeve. The jacketed test specimen was then instrumented with axial and radial cantilevers for strain measurement and installed in the pressure vessel for testing.

Table 1. Testing Matrix for BCH-3 Core Samples.

General Lithology	Depth Range (ft)	Core Analysis	XRD	Thin Section	TXC w/ UV @ 200 deg C	Thermal Expansion	Post-TXC Permeability
andesite	3567.25 – 3567.35	DEP1-1	DEP1-3	DEP1-2			
	3613.10 – 3613.20	DEP2-1	DEP2-3	DEP2-2			
rhyolite	3750.25 – 3750.35	DEP3-1	DEP3-3	DEP3-2			
	3899.00 – 3899.40	DEP4-4	DEP4-6	DEP4-5	DEP4-1, DEP4-2, DEP4-7, DEP4-8	DEP4-3	X
	4060.30 – 4060.40	DEP5-1	DEP5-3	DEP5-2			
	4127.15 – 4127.25	DEP6-1	DEP6-3	DEP6-2			
meta-volcanic	4209.15 – 4209.75	DEP7-1	DEP7-3	DEP7-2	DEP7-6, DEP7-7, DEP7-8, DEP7-9	DEP7-4	X
	4370.15 – 4370.25	DEP8-3	DEP8-2	DEP8-1			
	4486.20 – 4486.75	DEP9-1	DEP9-3	DEP9-2	DEP9-5, DEP9-6, DEP9-7, DEP9-8	DEP9-4	X
	4688.15 – 4688.70	DEP10-1	DEP10-3	DEP10-2	DEP10-5, DEP10-6, DEP10-7, DEP10-8	DEP10-4	X
	4863.00 – 4863.40	DEP11-7	DEP11-9	DEP11-8	DEP11-1, DEP11-2, DEP11-3, DEP11-4	DEP11-10	X

Core Analysis = Pulse or Pressure Decay Permeability, Bulk Density and Porosity;
XRD = X-Ray Diffraction, TXC = Triaxial Compression, UV = Ultrasonic Velocities

For failure characterization, suites of single-stage triaxial compression tests were conducted on vertical samples (i.e., samples aligned parallel to the borehole axis) to construct Mohr stress circles and calculate Coulomb parameters for both peak compressive strength corresponding to initial failure of the intact rock, and residual effective compressive strength corresponding to quasi-stable frictional sliding on the newly formed fracture at the end of each test. Triaxial compression tests were performed with air as the pore fluid and pore pressure drained to the atmosphere, and at temperatures of 200°C.

Summary of Rock and Mechanical Properties

The following tables list representative test results from the routine core analyses, uniaxial or unconfined compression stress tests (UCS) from the TSI™ scratch testing, triaxial compression tests, and Mohr-Coulomb failure evaluations for the lithotypes within selected core samples from the BCH-3 well. Table 2 lists the physical property measurements for all of the BCH-3 core samples, and Table 3 presents porosity and permeability relationships for selected samples. Table 4 represents a summary of the uniaxial compression tests along with derived parameters for the Mohr-Coulomb failure envelopes from the triaxial tests. Example UCS strength profiles for two metamorphic lithologies are shown in Figure 4.

In Table 4, the internal friction angles and internal linear cohesions are calculated by fitting a tangential line to the population of Mohr circles defined at the peak axial stresses when initial failure occurred for each confining pressure. The residual friction angles and residual cohesions represent the tangents to Mohr circles defined from the final, quasi-stable axial stress for each confining pressure. These residual friction angles, φ, are used to determine the coefficients of sliding friction, μ from the expression $\mu = \tan \varphi$. Example summary plots for the failure characterization in two metamorphic lithologies are shown in Figure 5.

At the nearby Desert Peak geothermal field, similarly-derived sliding friction values have been used in concert with two end-member 3D stress models to determine the propensity for frictional

Table 2. Core Analyses of BCH-3 Core Samples.

General Lithology	Sample ID	Depth (ft)	Ambient Porosity (%)	Dry Bulk Density (g/cc)	Grain Density (g/cc)	Steady-State Permeability	
						Net Effective Stress (MPa)	Gas Permeability (md)
andesite	**DEP 1-1**	3567.25	8.35	2.485	2.712	2.76	<0.01
	DEP 2-1	3613.10	9.72	2.448	2.712	2.76	<0.01
rhyolite	**DEP 3-1**	3750.25	10.16	2.393	2.664	2.76	<0.01
	DEP 4-4	3899.40	3.45	2.558	2.649	2.76	<0.01
	DEP 5-1	4060.30	8.76	2.386	2.615	2.76	<0.01
	DEP 6-1	4127.15	10.18	2.358	2.625	2.76	0.190
meta-volcanic	**DEP 7-1**	4209.45	2.34	2.699	2.764	2.76	<0.01
	DEP 8-3	4370.25	0.08	2.810	2.812	2.76	<0.01
	DEP 9-1	4486.20	0.63	2.772	2.790	2.76	<0.01
	DEP 10-1	4688.15	0.07	2.743	2.745	2.76	<0.01
	DEP 11-7	4863.30	0.47	2.785	2.798	2.76	<0.01

Table 3. Pre- and Post-test Permeability Relationships in BCH-3 Core Samples.

Well BCH Test Sample and Depth	General Lithotype	Pre-Test Ambient Porosity (%)	Pre-Test Pulse Decay Perm (md)	Pulse Decay Confining Conditions (psi, MPa)	Post-Test Pulse Decay Perm (md)*	Post-Test Perm/ Pre-Test Perm
DEP4 3899 ft	rhyolite	3.45	0.000184	1500, 10.34	2.126506	11,557
DEP7 4209 ft	meta-volcanic	2.34	0.000963	3000-4000, 20.68-27.57	0.055797	**58**
DEP9 4486 ft		0.63	0.000802	400, 2.76	0.159174	**199**
DEP9 4486 ft		0.63	0.000205	1500, 10.34	0.000010	**0.05**
DEP10 4688 ft		0.07	0.000638	400, 2.76	0.025422	**40**
DEP10 4688 ft		0.07	0.000249	1500, 10.34	0.000093	**0.37**

*Post-test permeability conducted on teflon-jacketed fractured core plugs.

Table 4. Uniaxial (UCS), Triaxial, and Mohr-Coulomb Properties, BCH-3 Core Samples.

Well BCH-3 Test Sample and Depth	General Lithotype	Average UCS (as calculated from TSI™ tests)		Mohr-Coulomb Properties*	
		(psi)	(MPa)	Sliding Friction Angle (degrees)	Coefficient of Sliding Friction
DEP4 3899 ft	rhyolite	35,000	241.4	41.3	0.8773
DEP7 4209 ft	meta-volcanic	16,000	110.3	43.7	0.9571
DEP9 4486 ft		40,000	275.9	40.3	0.8487
DEP10 4688 ft		28,000	193.1	29.1	0.5558
DEP11 4863 ft	meta-sedimentary	33,000	227.6	37.3	0.7632

*Derived from the Residual Effective Compressive Strength tests at 200° C.

failure along fractures seen in the stimulation interval from Well 27-15 as a function of excess fluid pressure (Hickman and Davatzes, 2010; Lutz et al., 2010). In this study at the Bradys geothermal field, the calculations from the mechanical tests are also being used to design optimal injection parameters for hydraulic stimulation during the Bradys EGS project.

Core Analyses

Core analyses from the BCH-3 core samples indicate high porosities (8-10%) but low permeabilities (<0.01 md) for the rhyolitic lithologies (Table 2). The sericitized top of the basement is characterized by Sample DEP7 (4,209 ft) that has 2.3% porosity but the rest of metamorphic core samples have less than 1% porosity and negligible permeability. Porosity in the Tertiary volcanic rocks is dominated by the matrix content. Crystal-rich ash flow tuffs such as Sample DEP4 have low ambient porosity values because they have a higher proportion of crystals to matrix. The XRD analysis of Sample DEP4 indicates 40% plagioclase crystals, and likely some of the quartz and potassium feldspar in the rhyolite are also present as solid crystals that displace the microporous devitrified matrix. Although dry grain densities are similar in the volcanic and metamorphic rocks, lower dry bulk densities in the volcanic rocks can be attributed to the higher porosities in the volcanics compared with the metamorphic rocks.

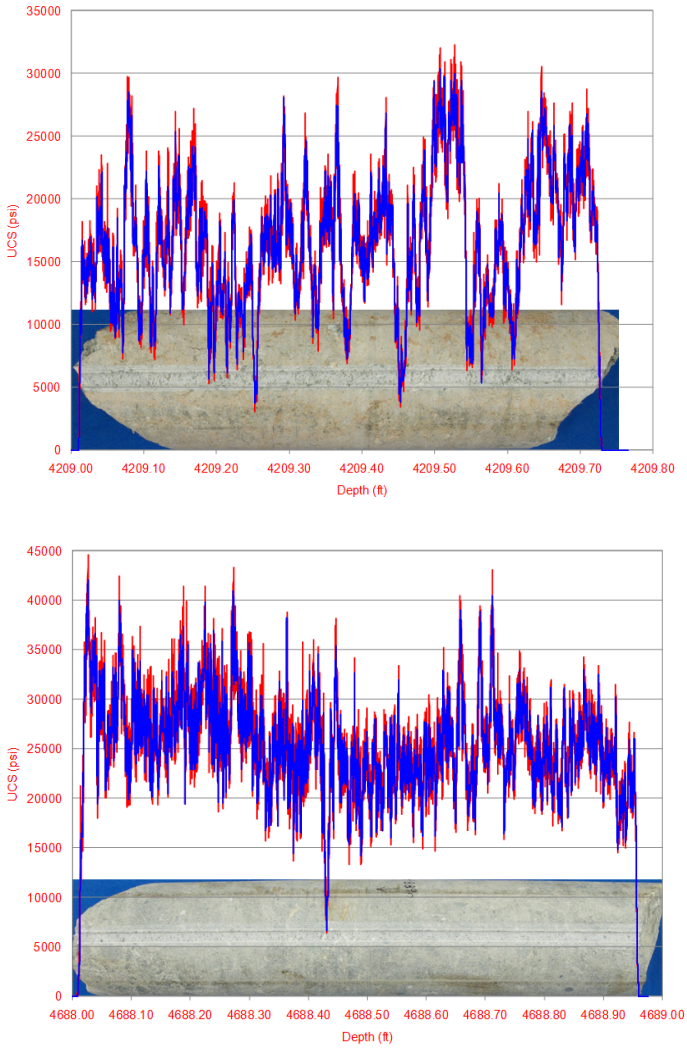

Figure 4. BCH-03 Samples DEP7 4209 ft (top) and DEP10 4688 ft (bottom). The raw data (red) and filtered data (blue, moving average) are superimposed over digital images of the core sections. In clast-supported meta-volcaniclastic rock of DEP7, Unconfined Compressive Strength (UCS) estimates range from approximately 4000 psi to 30,000 psi, and average approximately 16,000 psi (111 MPa). In chloritic meta-basalt of DEP10, UCS estimates range from approximately 6000 psi to 42,500 psi, and average approximately 28,000 psi (194 MPa).

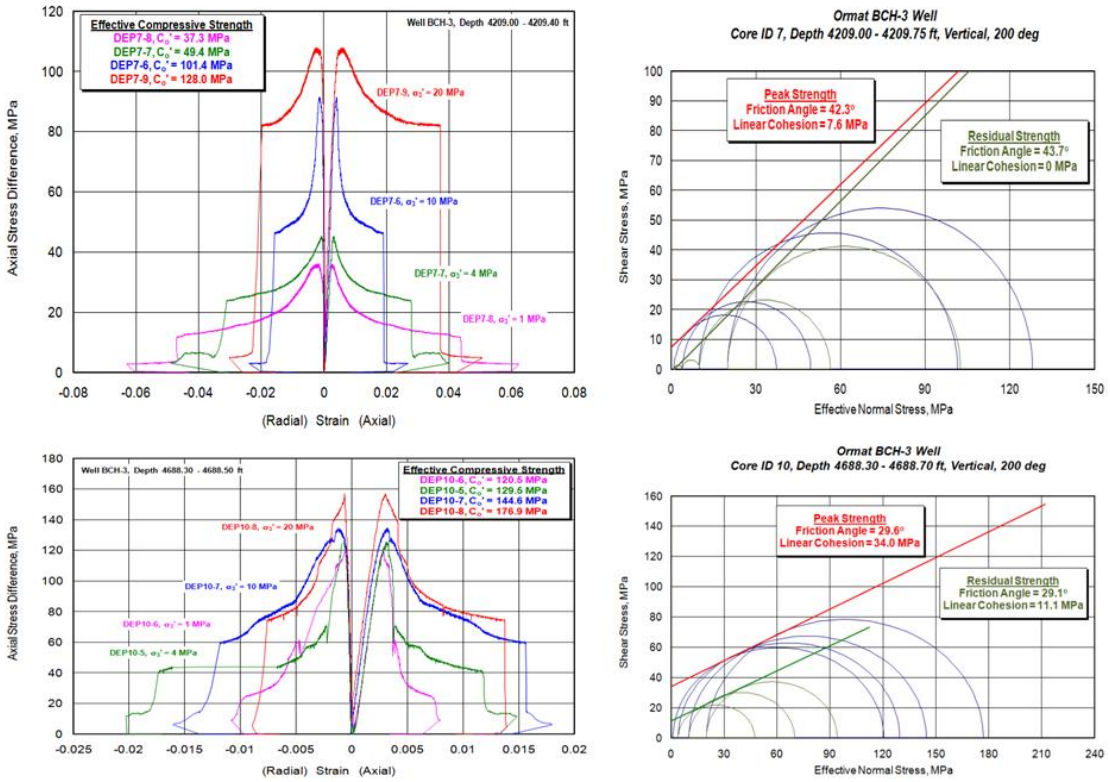

Figure 5. Triaxial compressive test results at a series of confining pressures (left) and Mohr stress circles with calculated Coulomb parameters (right) for Core Samples DEP7 4209 ft (top) and DEP10 4688 ft (bottom). Coulomb criteria (friction angle and linear cohesion) were determined for the entire test group.

Rock Mechanics Properties

Rock mechanical tests were conducted on the various lithologies to determine their mechanical properties including: stress-strain relationships, dynamic versus static Young's moduli, and frictional strengths and failure responses under a variety of thermal and confining conditions. The test results indicate moderately high rock strengths; with unconfined compressive strength (UCS) estimates of 240-275 MPa for the more siliceous lithologies, and 70-194 MPa for argillically-altered rhyolites and chloritic metavolcanic rocks. Because the high crystal content (>40%) supports the rock against compression, crystal-rich tuff in Sample DEP4 exhibits unexpectedly high UCS values, with an average of 241 MPa (Table 3). Meta-volcaniclastic rock represented by Sample DEP9 is clast-supported and also exhibits high UCS values with an average of 276 MPa.

Triaxial compressive tests were conducted on one rhyolite sample (DEP4) and four of the metamorphic core samples (DEP7, DEP9, DEP10, and DEP11). The triaxial compressive tests were conducted at 1, 4, 10 and 20 MPa confining pressures and at temperatures of 200°C. Effective compressive strengths range from 220 Mpa at 1 MPa confining pressure for the crystal-supported rhyolite (Sample DEP4), and 37 MPa at 1 MPa confining pressure for sericitized metamorphic rocks at the top of the basement (Sample DEP7), up to 304 MPa at 20 MPa confining pressure for pebbly meta-volcaniclastic rocks (Sample DEP9). The results of the triaxial tests indicate that the crystal-supported rhyolites (Sample DEP4) and clast-supported meta-volcanics (Sample DEP9) show less of a change in strength at increased confining pressures than do the more argillaceous lithologies. The weaker argillaceous rocks start out at low values and then compact at higher confining pressures to become stiff at higher rates than do the already well-supported rocks.

Residual compressive strengths range from 3.8 MPa at 1 MPa confining pressure in sericitized metamorphic rocks (Sample DEP7) to 103 MPa at 20 MPa confining pressure in crystal-rich rhyolite tuff (Sample DEP4). Quasi-static values for Young's moduli range from 48 to 55 GPa (in crystal-rich rhyolite tuffs) up to 60-76 GPa (in the metamorphic rocks); Poisson's ratios range from 0.10 to 0.29. Based on the results of compression strength testing, the stiffer siliceous rocks generally display higher Young's modulus values. The strongest rocks in the sample suite appear to be the highly metamorphosed, partially siliceous meta-sediments (Sample DEP11 at 4,863 ft). Although the XRD analysis of Sample DEP11 indicates 55% total clay, this sample has the highest quartz content of the rock mechanics samples, with 36% quartz. The quartz content of the microcrystalline matrix apparently supports the rock against compressive stress despite the high clay content.

The results of the laboratory tests were used to construct Mohr-Coulomb failure envelopes for the proposed reservoir rocks, and to evaluate the propensity for frictional failure along natural fractures in the open-hole interval of Well 15-12. At 200°C, sliding friction angles for the residual effective compressive strength range from 29.1° to 43.7° (Table 4). Corresponding coefficients of sliding friction values range from 0.56 in chlorite-altered meta-basalt (Sample DEP10 at 4,688 ft), up to 0.98 in clast-supported meta-volcaniclastic rocks (Sample DEP9 at 4,486 ft). In thin section, Sample DEP10 appears to represent an originally glassy amygdular to fragmental basalt where all of the the original glass has converted to chlorite. XRD analysis of Sample DEP10 indicates 51% chlorite and 61% total clay in the meta-basalt. The high clay content and low coefficient of sliding friction for this sample suggests a high propensity for frictional failure in this type of rock.

The argillaceous volcanic and sericitized metamorphic rocks have the highest initial porosities, with 10% ambient porosity recorded for the devitrified rhyolites. Comparison of pre- and post-test core data appears to indicate up to a 200-fold increase

in permeability as a result of dilational failure in originally tight (<1% porosity) argillaceous meta-volcanics (Table 3). However, the methods used to determine permeability on the jacketed post-test core plugs cannot distinguish gas flow through the rock from flow around the outside of the fractured sample, and the amount of increased permeability should be considered especially qualitative.

Summary

Systematic sampling and XRD analyses of the Well 15-12 cuttings reveals well-defined hydrothermal alteration zones in clay and zeolite minerals in Tertiary volcanic units overlying metamorphic basement rocks. The upper alteration zone is characterized by low-temperature alteration minerals: smectite clay; clinoptilolite zeolite alteration, and iron-bearing carbonate (ankerite, siderite) veins. The argillic alteration zone extends to a depth of 2,100 ft, where epidote-bearing wallrock alteration and fault gouge indicate the presence of exhumed footwall rocks along a large-displacement normal fault (likely the subsurface projection of the Bradys Fault mapped at the surface). Below the fault, there is a sharp change to mixed-layer illite-smectite (I/S clay) and laumontite veins and amygdule-fillings in Miocene basaltic andesite flows.

Devitrified rhyolite ash flow tuffs are present from 3,700 ft to the top of the basement at about 4,000 ft. The tuffs are slightly to moderately siliceous and clay-altered. Illite-smectite clays in the tuffs have 20-30% smectite interlayers. With depth, there is a consistent decrease in the amount of interlayered smectite in the I/S clay that is related to paleo-temperatures in the Bradys geothermal history. At the top of the I/S zone at 2,400-2,900 ft, the mixed-layer clay is smectite-rich with up to 60% smectite interlayers, indicating formation of the I/S clay at about 180°C. Closer to the basement contact, the I/S clay has 20-30% smectite interlayers, suggesting slightly higher paleo-temperatures in the 180-200°C range. I/S clays persist in the upper part of the basement from the contact at about 4,000 ft to approximately 4,800 ft.

Below the sericitized top, metamorphic rocks in the basement are composed of hematitic metavolcanics and chloritic volaniclastic meta-mudstones associated with the Jurassic Humboldt Mafic Complex. These rocks are moderately siliceous, weakly propylitically altered, complexly veined, and moderately deformed. Well 15-12 has 850 feet of open hole in these competent, fractured rocks with sub-commercial permeability, to a total depth of 5,096 ft. The metamorphic rocks in the open hole interval have abundant veins, clayey shear planes, and other planar features that may be amenable to shear stimulation under higher wellhead fluid pressures. Hydraulic stimulation of the well is intended to enhance formation permeability through self-propping shear failure along the most optimally oriented and critically stressed of these pre-existing features. In the metamorphic rocks, high clay contents and low coefficients of sliding friction determined from the mechanical tests suggest a high propensity for frictional failure.

Acknowledgements

The Bradys EGS project is supported by the U.S. Department of Energy, Assistant Secretary for Energy Efficiency and Renewable Energy, under DOE Grant No. DE-FC36-08GO18200/001.

References

Benoit, W.R., J.E. Hiner, and R.T Forest, 1982, Discovery and Geology of the Desert Peak Geothermal Field: A Case History, Nevada Bureau of Mines and Geology Bulletin 97, 82p.

Davatzes, N. and Hickman, S., 2009, Fractures, stress, and fluid flow prior to stimulation of Well 27-15, Desert Peak, Nevada, EGS Project: Proceedings, Thirty-Fourth Workshop on Geothermal Reservoir Engineering Stanford University, Stanford, California, 9-11 February, SGP-TR-187.

Faulds, J.E. and Garside, L.J., 2003, Preliminary geologic map of the Desert Peak – Brady geothermal fields, Churchill County, Nevada: Nevada Bureau of Mines and Geology Open-File Report 03-27.

Faulds, J.E., Garside, L., and Oppliger, G.L., 2003, Structural analysis of the Desert Peak-Brady Geothermal Fields, northwestern Nevada: Implications for understanding linkages between northeast-trending structures and geothermal reservoirs in the Humboldt structural zone: Geothermal Resources Council Transactions, v. 27, p. 859-864.

Faulds, J.E., and Hinz, N.H., 2003, Bradys-Desert Peak Core Logs, Nevada Bureau of Mines and Geology.

Hickman, S. and Davatzes, N., 2010, In-situ stress and fracture characterization for planning of an EGS stimulation in the Desert Peak geothermal field, NV Proceedings, Thirty-fifth Workshop on Geothermal Reservoir Engineering Stanford University, Stanford, California, 1-3 February, SGP-TR-188.

Johnson, D.A., and Barton, M.D., 2000, Time-space development of an external brine-dominated, igneous-driven hydrothermal system: Humboldt Mafic Complex, Western Nevada: Part 1. Contrasting Styles of Intrusion-associated Hydrothermal Systems, Dilles, Barton, Johnson, Proffett, Einauldi, eds., Society of Economic Geologists Guidebook Series, Volume 32, p. 127-143.

Lutz, S.J., Hickman, S., Davatzes, N., Zemach, E., Drakos, P., and Robertson-Tait, A., 2010, Rock mechanical testing and petrologic analysis in support of well stimulation activities at the Desert Peak geothermal field, Nevada: Proceedings, Thirty-fifth Workshop on Geothermal Reservoir Engineering Stanford University, Stanford, California, 1-3 February, SGP-TR-188.

Lutz, S.J., and J.B. Hulen, 2002, Geologic setting and alteration mineralogy of the Nickel mine and Bolivia region, Jurassic Humboldt Mafic Complex and Boyer Ranch Formation, northern Stillwater Range, Nevada: Geological Society of Nevada Spring 2002 Field Trip Guidebook, Special Publication No. 35, Jurassic Magmatism and Metal Deposits in Western Nevada, p. 117-133.

Lutz, S.J., Moore, J.N., Jones, C.G., Suemnicht, G., and Robertson-Tait, A., 2009, Geological and structural relationships in the Desert Peak geothermal system, Nevada: Implications for EGS development: Proceedings, Thirty-fourth Workshop on Geothermal Reservoir Engineering Stanford University, Stanford, California, 9-11 February, SGP-TR-187.